A Petrological and Geochemical Account of Subsurface Noritic Intrusion in the Western Part of Bundelkhand Massif, Shivpuri District, M.P.

Madhuparna Roy[*], Pradeep Pandey, Shailendra Kumar and R. P. Singh

Atomic Minerals Directorate for Exploration and Research, West Block-7, R.K.Puram, New Delhi - 110 066
*E-mail: madhuparnaroy.amd@gov.in

ABSTRACT

Subsurface exploration for uranium in the northwestern part of Bundelkhand massif, near Khor area, Shivpuri dist., M.P., resulted in intercepting a substantial thickness of mafic rock within Bundelkhand granitoid. Intercepts of this mafic rock at various levels in the boreholes, indicate that the rock mainly occurs as dyke-like intrusion and fracture-fills within Bundelkhand granite. It is essentially composed of hypersthene and plagioclase, with or without olivine, leading to the characterisation as hypersthene microdolerite, noritic dolerite and norite (±olivine), depending on the grainsize and variation from intergranular to ophitic texture. Chemically, the rock is characterised by av. 49.09% SiO_2, 2.46% TiO_2, 2.33 Fe_2O_3, 9.45% FeO, 5.75% MgO, 8.37% CaO and 0.96% K_2O. The normative composition ranges from 3.53% quartz, 46.86% plagioclase, 12.58% diopside, 19.24% hypersthene. The olivine normative samples show av. 5.65% olivine. Geochemical plots indicate an intra-plate affinity along with oceanic signature, while presence of mineralogical and normative olivine, together with the REE pattern, point towards a lower crustal or mantle source. The mineralogical and normative presence of either quartz or olivine in these mafic rocks implies that it has an intermediate character between the tholeiitic dolerite dykes and the komatiite-type ultramafics reported from Bundelkhand craton. The complex geochemical signature of the rocks also reveals that both intra-continental as well as a mixture of oceanic- to upper mantle signatures are evident. The present study is a first time report of the occurrence of this hitherto unknown noritic body at depth within the Bundelkhand granite, which has no visible surface expression. The findings may strengthen the existing concept of a continuum between Rajasthan craton in the west and Bundelkhand craton in the east, as a single proto-continent.

INTRODUCTION

The Bundelkhand massif is considered to be part of the larger Rajasthan-Bundelkhand craton (Sharma, 2009), with the two cratonic blocks, separated by a vast tract of Vindhyan cover rocks over a distance of a few hundred kilometers, beside the Great Boundary Fault marking the eastern limit of the Rajasthan (Banded Gneissic Complex (BGC)-Berach granite) block. The Bundelkhand massif comprises supracrustals of TTG gneisses, metavolcano-sedimentary rocks and syn- to post tectonic granitoids that marked the stabilization of the craton. The craton is flanked on the west by the Proterozoic rocks of the Vindhyan Supergroup that conceal the continuity of Berach granite of Rajasthan in the west from Bundelkhand granitoid in the east, thus rendering geological correlation obscure. The Rajasthan block comprises Archean basement of polymetamorphosed and multi-deformed gneisses, migmatites, granitoids and amphibolites (BGC), over which Proterozoic cover rocks of the Aravalli and Dehi Supergroup were deposited, much after the stabilization of the craton. It also contains Proterozoic carbonatitic and granitic rocks and old granulites and norites within Delhi metasediments, mainly at Sandmata. The two blocks are also believed to have similar lithology, deformational events, dyke activity, geochronological ages (Meert et al., 2010) and geodynamic settings defined by similar geochemistry of mafic igneous rocks (Mondal and Ahmad, 2001). In view of this, it is believed that the two cratons evolved as a single large protocontinent, to the north of the Son-Narmada lineament, that stabilized around 2.5Ga years ago.

The present study pertains to extensive examination of sub-surface samples from the western part of Bundelkhand craton, near Khor area, Shivpuri dist., M.P. It brings to light hitherto unreported occurrence of mafic intrusive rocks of noritic affinity without any visible surface expression, within Bundelkhand granitoid, and which possibly corroborates similar noritic activity observed in Rajasthan block in the west.

REGIONAL AND LOCAL GEOLOGY

The Bundhelkhand craton constitutes a semi-circular outcrop stretching over 26,000 sq km in parts of central Indian shield and is marked by the Bundhelkhand massif comprising Archaean to early Proterozoic gneisses-migmatites, mafic-ultramafic rocks and granitoids of different episodes. The entire suite is intruded by quartz reefs and dolerite dyke swarms of tholeiitic affinity, succeeded by early Proterozoic Bijawar and Gwalior Groups of sediments in the south-southeast and northwest of the massif respectively, overlain by Vindhyan super Group of rocks.

In the northwestern part of Bundelkhand massif, lies Khor area (25°14'16": 77°57'57"; Toposheet No. 54 G/16), Shivpuri district, M.P., which lies about 20km SW of Mohar caldera, (Fig.1) marking the western limit of the massif in this part, beyond which Vindhyan Supergroup unconformably overlie the basement Bundelkhand granitoids. The Vindhyans in Khor area is represented by a veneer of ~25-30m undeformed, subhorizontal, cross-bedded, ferruginous sandstone-shale of Kaimur Group. The basement, on the other hand, comprises variants of granitoids, ranging from fine to coarse, biotite bearing pink and grey granitoids.

LITHOLOGY

Subsurface geology of this area was largely unravelled by lithololoical, petrological and geochemical studies of drill core samples. The study shows that stratigraphically, the rock types fall under three main groups, in this order (a) basement Bundelkhand granitoid with its older supracrustal enclaves (b) younger mafic rocks intrusive into the granitoid and (c) the youngest Kaimur Group. The basement Bundelkhand granitoid comprises light pink coloured,
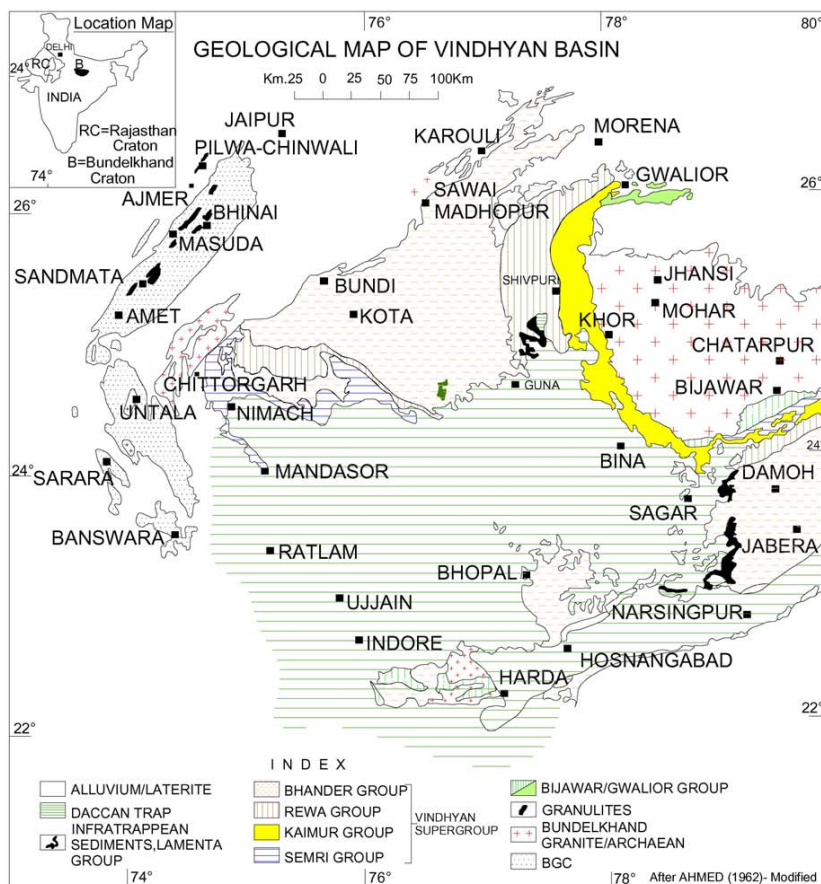
Fig.1. Location of Khor area with respect to Bundelkhand and Rajasthan cratons.

feldspathic sandstone with thin intercalations of purple shale and clast-supported, fine sandstones and pink silty shale. The Kaimur sediments overlie the basement granitoid across an unconformity surface that is marked by up to 75cm thick pebbly/conglomeratic beds with quartz, feldspar and chert pebbles forming distinct regolith.

PETROGRAPHY OF MAFIC ROCK

Irrespective of depth, the mafic rocks are composed dominantly of plagioclase, orthopyroxene (hypersthene), subordinate clinopyroxene (diopside), major magnetite-ilmenite and accessory apatite. Olivine is present in a few samplesis characterised by pale to dark olive green color, high R.I, high order interference color and alteration character. Hypersthene is characterised by faint to distinct, pink to pale green pleochroism, typical pyroxene cleavage, lower second order interference color and straight extinction. On the basis of the presence of hypersthene (± olivine) and plagioclase as essential minerals and the varying grain size apparent megascopically in core samples (Fig.4a,b,c,d), these mafic rocks are characterised as hypersthene-olivine microdolerite at shallower levels, noritic (± olivine) dolerite (synonymous to gabbroic dolerite) at the intermediate levels and norite (± olivine) at the deeper levels. The mafic rocks at the shallower levels are very fine to medium grained and characterized by typical doleritic/intergranular texture defined by interlocking plagioclase laths enclosing fine pyroxene in triangular interstitial spaces. At places, the texture is microporphyritic with conspicuous

medium to coarse, at places aplitic, foliated chlorite-/ biotite granite with alteration signatures like chloritisation, silicification and ferruginisation. This is intruded by dark green, medium grained, hard and compact mafic rock (Fig.2), which also occupies available fracture planes within the granitoid, as it is intercepted at various levels in different boreholes (Table 1). Sharp contact with the granite noted during core examination (Fig 3), implies its intrusive nature. The incidence of these mafic rocks at various levels together with their observed characters (grain size, mineralogy and texture), suggest that the shallower intrusions are part of the same mafic body at depth, and signify injections along fractures at various shallow- to intermediate levels within the host granite. According to the bore hole data the thickness of the mafic body is greater in the NW and SE directions. The Kaimur Group is represented by fine to medium grained, clast / matrix supported, well sorted, bedded, hard and compact, variegated,

Table 1. Depth range of mafic rock intrusive into basement granite (Reduced Level(RL) of borehole collar : 416.76 – 423.97m;DD: Drilled depth)

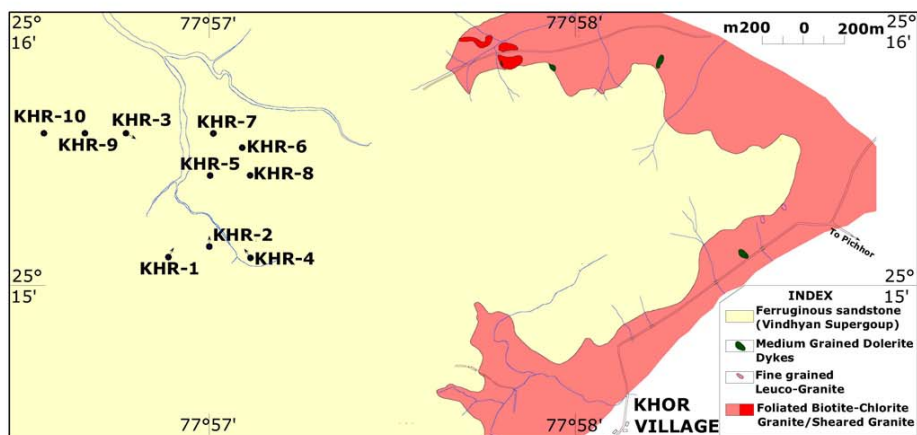| Borehole No.	Depth Range		
	1 (m)	2 (m)	3 (m)
KHR-1	167.50 -168.35 177-181.40	277.85-295.10 (DD)	
KHR-2	207.65-215.20	265.90-273.80	286-360.50 (DD)
KHR-3	-	245-305.15 (DD)	
KHR-4	182.92-183.30 185.75-189.60	222.25-310.65 (DD)	
KHR-5(V)	-	242.25-300.45 (DD)	
KHR-6(V)	66 - 81	265.80-300.05 (DD)	
KHR-7(V)	177.45-194.40		
KHR-8(V)	-	255.25-305.05 (DD)	
KHR-9(V)			216.30-300.25 (DD)
KHR-10(V)			227.10-300.30 (DD)

Fig.2. Geological map with location of boreholes, Khor area, Shivpuri dist., M.P.

Fig.3. Sharp contact of mafic rock at the top of granite. KHR-1/168.35

Fig.4. (a) Olivine (micro) dolerite KHR- 10/216.40. **(b)** Hypersthene dolerite KHR-4/227.15. **(c)** Olivine norite KHR-10/300.00. **(d)** Norite KHR-5/299.00.

subhedral microphenocrysts of green to brown olivine (Fig 5a) and colorless laths-shaped crystals of plagioclase embedded in a finer groundmass of plagioclase, pyroxene (±olivine) and abundant fine ilmenite (+magnetite). Often olivine is mantled by brown rim of iddingsite and other alteration products. The mafic rocks at deeper levels are generally coarser grained, composed of coarse (a few mm across) hypersthene (+subordinate clinopyroxene), poikilitically (sub-ophitic/ophitic) enclosing finer plagioclase laths (Fig.5b,c). Unlike most norites where both plagioclase and hypersthene are coarse in nature, these rocks contain coarse pyroxene and fine plagioclase. In most coarse grained sample interstitial quartz is observed (Fig.5d). In rare cases remnant of olivine (Fig.5e) is noted in the norite and such samples do not contain quartz. Grain-size variation of the mafic rocks (Fig.5f) with depth in the bore hole is shown in Plate 1.

Presence of Olivine and Quartz

Euhedral to subhedral olivine microphenocrysts are more conspicuous in the finer variety than in the coarser one and may represent early crystal fraction, squeezed in forcefully through fractures and fissures of the granitoid. In the coarser variants, olivine is present in traces as remnant grains, along with the predominant orthopyroxene and plagioclase. All this, combined with the fact that the olivine containing rocks are found at different structural levels, may indicate the role of fractional crystallisation, whereby, the earlier crystallised olivine grains may not have had sufficient time to react with the main residual melt in order to get fully converted to orthopyroxene. This may result in the melt getting enriched in silica, reflected by the presence of interstitial quartz along with orthopyroxene in other samples. Minor- to trace amount of symplectic/granophyric or anhedral quartz noted in the interstices of major minerals in the coarse grained samples may be attributable to this.

Textural Interpretation

The fineness of grainsize and consequent texture of the micro-dolerite is possibly the result of rapid chilling near its contact with the colder granite as the hot melt made its way through fractures at shallow levels. However, the presence of microphenocrysts of olivine in a fine plagioclase rich groundmass in some parts of the microdolerite may be due to forceful injection of the melt which entrailed the already crystallized olivine crystals from the deeper part of the magma chamber to the shallower level. A compositional difference is also noticed between the shallower microdolerite and the deeper norite, with the former being enriched in olivine and the latter in plagioclase (+OPx) and some amount of quartz.
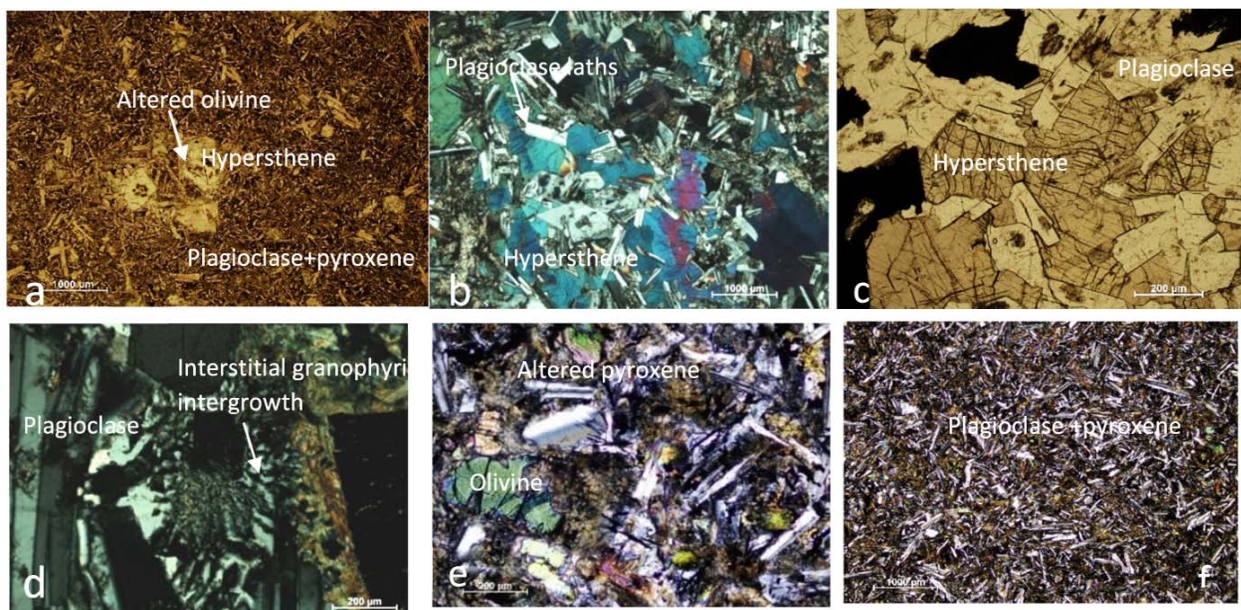

Fig.5. (a) View of altered olivine (KHR-1/177) in olivine microdolerite. **(b)** Texture of norite. KHR-3/276. **(c)** Granophyric quartz in the interstices of norite. KHR-3/303.15. **(d)** Hypersthene and plagioclase in coarse grained norite. KHR-3/30.2 **(e)** Remnant of olivine in norite, KHR-10/227.80. **(f)** Texture of hypersthene dolerite. KHR-5/293
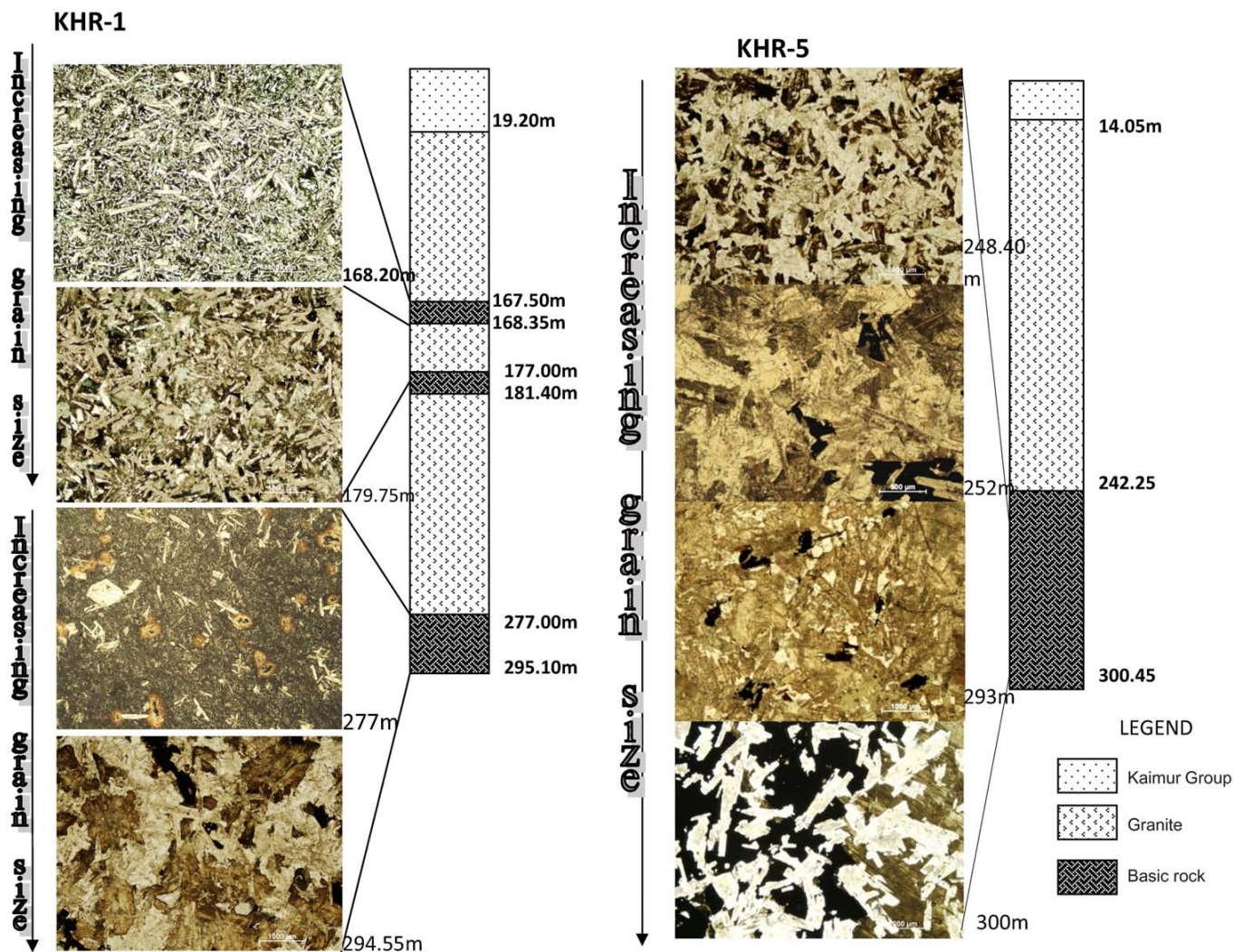
Plate 1. Grain size variation of mafic rock with depth (not to scale). all photomicrographs under the same magnification; bar=1000μ
White laths : plagioclase; Dark mineral: pyroxene; Opaque: Magnetite-ilmenite.

Major Mineral Paragenesis

Dolerite: Plagioclase crystallization predominated during major part of the crystallization history, followed by interstitial pyroxene (± olivine), opaques and quartz. Opaques overlap with pyroxene in crystallization sequence.

Plagioclase
    Pyroxene
        Magntite-ilmenite
            Quartz
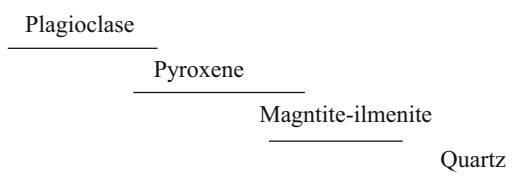
Norite : Plagioclase crystallization prevailed throughout, at first on a lower scale (explaining lesser poikilitic inclusion of plagioclase in pyroxene, by volume), followed by more prolific and continued crystallization of post-pyroxene plagioclase. The opaques overlapped with pyroxene and quartz formed last.

Plagioclase
  Olivine
      Pyroxene
         Magnetite-ilmenite
            Quartz
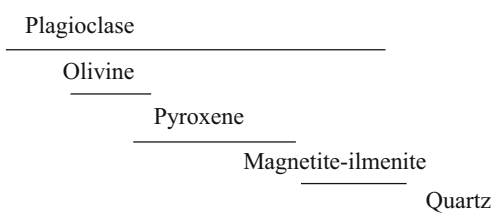
GEOCHEMISTRY

Geochemical analyses of samples were carried out by spectro-photometry (SiO_2, TiO_2 and P_2O_5), atomic absorption spectro-metry (Al_2O_3, Fe_2O_3, MnO, MgO, CaO, Ni, Co, Cr, Ba, Rb, Sr)), flame photometry (Na2O, K2O), titrimetry (FeO) and gravimetry (LOI). Rare Earth Elements, Y, Zr, V, Sc, Nb were analysed by inductively coupled plasma-optical emission spectrometry. Major, minor and trace element data (n=26) of the noritic rocks are givenn in Table 2 and 3. It is seen that the composition of all the samples is broadly consistent. Mafic index of the rocks vary from 54.80 to 76.77 and Larsen's index from -10.7 to 3.9. Normative composition of the suite (Table 4) shows that most of the samples contain quartz (upto 12.29%; av. 3.53%) and diopside (0.12-21.365; av.12.58%) with a few having corundum (av. 0.68%), in addition. Hypersthene is the ubiquitous component in most samples constituting 6.36-32.17%, apart from invariable plagioclase (36.72-57.12%; av.46.86%). Several samples contain 0.53-18.97% (av. 5.65%) normative olivine. Average normative 4.68% ilmenite and 3.41% magnetite also corroborate the observed ore mineralogy. Binary plots of SiO_2 vs major oxide (Plate-2a) show that the composition of the suite is fairly consistent. Plots of major oxides vs Larsen's index (Plate-2b) shows variation of Al_2O_3, MgO, CaO, Na_2O and K_2O with Larsen's Index. Plot of SiO_2 vs Na_2O+ K_2O (Plate-2c) indicates that the suite mostly plots in the sub-alkaline, gabbro to gabbroic diorite fields. On the Zr vs P_2O_5 (Plate-2d) and Zr/P_2O_5 vs Nb/Y

Table 2. Major and minor oxide data (%) of mafic rocks of Khor by Spectrophotometry, AAS, Flame photometry, Titrimetry and Gravimetry (n=26).(Mg#: Mg number; MI: Mafic index; LI: Larsen's index)

	SiO₂	TiO₂	Al₂O₃	Fe₂O₃	FeO	MnO	MgO	CaO	Na₂O	K₂O	P₂O₅	LOI	Mg#	MI	LI
KHR-1/179.75	47.10	2.47	14.9	2.75	8.44	0.2	7.11	7.24	2.7	1.66	0.31	4.53	60.01	61.15	-5.43
KHR-1/239.80	52.90	1.16	16.2	3.96	4.54	0.08	7.01	4.74	3.03	2.41	0.45	2.83	73.34	54.80	3.75
KHR-1/294.55	48.00	2.81	14.7	1.5	9.99	0.14	7.09	8.57	2.86	0.75	0.28	3.15	55.84	61.84	-8.90
KHR-2/268.20	53.04	1.90	11.59	1.19	11.06	0.11	5.97	7.99	2.18	0.38	0.17	1.93	49.02	67.23	-6.96
KHR-3/248.40	49.20	2.85	13.90	2.04	9.73	0.13	6.12	9.06	1.68	0.60	0.22	4.09	52.84	65.79	-7.91
KHR-3/276.05	49.20	2.45	16.10	1.52	9.09	0.12	4.88	9.67	3.03	0.90	0.26	2.16	48.89	68.50	-6.34
KHR-3/303.15	48.00	3.05	17.20	2.02	9.88	0.13	3.72	10.18	3.03	0.60	0.32	1.83	40.15	76.18	-7.18
KHR-4/227.15	49.50	2.03	16.50	2.65	7.59	0.12	6.35	7.88	2.70	1.51	0.36	2.49	59.85	61.72	-3.81
KHR-4/302.80	49.70	2.57	18.20	1.02	8.66	0.12	4.56	8.10	2.70	1.21	0.27	2.82	48.40	67.98	-3.54
KHR-5/252.20	47.40	2.41	16.40	2.85	8.66	0.14	6.97	5.89	2.53	1.21	0.22	4.86	58.91	62.28	-4.51
KHR-5/293.00	48.00	2.65	16.20	2.10	8.23	0.12	7.48	6.16	2.36	1.66	0.28	4.67	61.82	58.00	-4.21
KHR-6/114.10	49.60	2.52	15.40	1.45	9.88	0.14	5.89	8.47	2.53	0.90	0.26	2.80	51.51	65.80	-6.81
KHR-6/276.45	49.80	2.66	15.40	1.35	9.95	0.14	5.62	8.92	2.53	0.90	0.29	2.18	50.16	66.78	-6.99
KHR-6/300.05	49.10	2.87	16.90	1.05	10.3	0.14	4.50	8.62	2.86	0.75	0.32	2.08	43.77	71.61	-6.30
KHR-7/226.90	42.50	2.88	18.40	1.96	9.56	0.25	5.71	6.75	2.70	1.81	0.33	6.97	51.55	66.86	-6.04
KHR-8/259.50	45.70	2.85	17.40	3.52	8.37	0.16	5.67	7.54	2.53	0.90	0.24	4.73	54.69	67.71	-5.45
KHR-8/264.80	47.40	2.46	15.90	3.26	10.20	0.15	5.65	8.85	2.69	0.75	0.21	1.97	49.67	70.43	-8.15
KHR-9/216.40	48.40	2.51	12.65	7.58	5.84	0.15	6.26	10.34	2.21	0.48	0.27	0.69	65.63	68.19	-5.83
KHR-9/229.05	48.87	3.22	11.87	2.51	12.02	0.15	5.30	9.09	1.7	0.77	0.34	1.53	44.00	73.27	-9.35
KHR-9/257.65	46.57	2.95	13.34	2.38	12.29	0.13	4.44	9.30	2.14	0.55	0.35	2.89	39.16	76.77	-9.96
KHR-9/299.70	56.26	1.21	12.96	2.77	6.92	0.08	3.93	5.92	2.95	1.92	0.14	2.41	50.29	71.15	3.90
KHR-10/218.80	50.54	2.29	13.27	1.49	10.89	0.18	7.97	8.32	0.47	0.46	0.31	1.41	56.60	60.84	-9.87
KHR-10/227.25	49.42	2.33	12.65	0.91	11.6	0.15	6.59	9.56	2.99	0.50	0.33	1.53	50.30	65.50	-10.8
KHR-10/237.80	50.55	2.46	12.57	0.69	11.03	0.15	5.75	10.04	2.13	0.50	0.32	1.28	48.15	67.09	-9.47
KHR-10/270.0	49.29	2.68	13.18	2.52	12.16	0.14	4.77	9.54	2.14	0.46	0.22	1.61	41.14	75.48	-9.58
KHR-10/300.0	50.42	1.82	14.05	3.66	8.79	0.12	4.26	10.82	2.13	0.46	0.16	1.04	46.34	74.51	-6.60
MAX	56.26	3.22	18.40	7.58	12.29	0.25	7.97	10.82	3.03	2.41	0.45	6.97	73.34	76.77	3.90
MIN	42.50	1.16	11.59	0.69	4.54	0.08	3.72	4.74	0.47	0.38	0.14	0.69	39.16	54.80	-10.7
Av	49.09	2.46	14.92	2.33	9.45	0.14	5.75	8.37	2.44	0.96	0.28	2.71	52.00	67.21	-6.24

Table 3. Trace element data (ppm) of mafic rocks of Khor by ICP-OES and AAS (n=26)

	Ni	Co	Cr	Ba	Rb	Sr	Zr	V	Sc	Nb
KHR-1/179.75	98	46	155	210	66	182	280	246	24	19
KHR-1/239.80	50	<25	60	801	84	549	275	135	14	14
KHR-1/294.55	71	47	82	175	<25	213	216	299	25	22
KHR-2/268.20	71	45	165	148	10	123	148	175	NA	13
KHR-3/248.40	80	44	168	196	37	191	213	226	24	19
KHR-3/276.05	77	31	103	191	27	237	205	232	22	21
KHR-3/303.15	73	14	42	154	<25	228	220	257	20	23
KHR-4/227.15	65	37	114	404	54	322	248	210	21	17
KHR-4/302.80	58	34	59	198	36	229	219	216	20	21
KHR-5/252.20	77	48	166	206	35	189	209	241	23	18
KHR-5/293.00	79	30	122	218	48	169	209	236	23	20
KHR-6/114.10	163	39	141	176	33	193	200	244	22	19
KHR-6/276.45	99	46	100	213	29	200	226	256	24	22
KHR-6/300.05	99	42	65	174	<25	238	210	257	22	23
KHR-7/226.90	70	32	64	305	63	193	235	269	24	23
KHR-8/259.50	77	36	138	207	29	190	239	267	25	22
KHR-8/264.80	98	39	194	207	27	197	213	242	22	19
KHR-9/216.40	135	86	185	202	16	194	199	282	NA	20
KHR-9/229.05	92	69	68	226	35	187	242	334	NA	29
KHR-9/257.65	87	64	73	276	38	220	268	288	NA	25
KHR-9/299.70	62	43	30	370	54	194	124	193	NA	14
KHR-10/218.80	197	48	308	174	65	154	191	274	NA	28
KHR-10/227.25	140	53	260	222	29	193	238	274	NA	20
KHR-10/237.80	96	54	177	226	79	202	220	278	NA	20
KHR-10/270.00	93	64	67	191	33	199	197	264	NA	22
KHR-10/300.00	79	49	41	143	34	228	184	196	NA	16
Max	197	86	308	801	84	549	280	334	25	29
Min	50	14	30	143	10	123	124	135	14	13
Av	91.77	45.60	121.04	238.96	41.78	215.92	216.46	50.00	22.19	20.35

Table 4. Normative data (%) of mafic rocks of Khor, (n=26)

	Quartz	Plagioclase	Orthoclase	Corundum	Diop.	Hypersth	Olivine	Ilm.	Mag.	Apatite
KHR-1/179.75	0	46.41	9.96		8.43	14.22	6.47	4.69	3.99	0.72
KHR-1/239.80	4.68	46.38	14.9	0.89		20.77		2.20	5.74	1.04
KHR-1/294.55	0	49.18	4.58		2.92	15.90	5.97	5.34	2.17	0.65
KHR-2/268.20	9.86	39.16	2.25		14.35	24.13		3.61	1.73	0.58
KHR-3/248.40	6.98	42.76	3.69		12.32	20.91		5.41	2.96	0.51
KHR-3/276.05	0	53.24	5.46		15.49	14.11	1.47	4.65	2.20	0.6
KHR-3/303.15	0	57.12	3.69		14.18	13.16	0.53	5.79	2.93	0.74
KHR-4/227.15	0.3	51.11	9.29		6.97	21.05		3.86	3.84	0.83
KHR-4/302.80	1.71	56.74	7.30		4.08	20.39		4.88	1.48	0.51
KHR-5/252.20	1.04	49.24	7.30	0.70		27.19		4.58	4.13	0.51
KHR-5/293	0.04	48.60	9.96		0.12	27.80		5.03	3.04	0.65
KHR-6/114.10	1.83	49.34	5.46		10.25	22.67		4.79	2.10	0.6
KHR-6/276.45	2.01	49.34	5.46		11.95	21.13		5.05	1.96	0.67
KHR-6/300.05	1.09	55.19	4.58		8.13	20.73		5.45	1.52	0.74
KHR-7/226.90	0	52.55	10.91	0.46			18.97	5.47	2.84	0.76
KHR-8/259.50	0.33	54.80	5.46		2.03	21.19		5.41	5.1	0.56
KHR-8/264.80	0	51.78	4.58		11.17	18.16	1.95	4.67	4.73	0.49
KHR-9/216.40	8.26	41.88	2.84		21.11	6.36		4.77	10.99	0.39
KHR-9/229.05	7.11	36.87	4.55		17.52	19.54		6.12	3.64	0.63
KHR-9/257.65	3.2	43.28	3.25		15.71	19.15		5.60	3.45	0.79
KHR-9/299.70	12.29	41.14	11.35		9.89	13.48		2.30	4.02	0.32
KHR-10/218.80	11.19	36.72	2.72		6.63	32.17		4.35	2.16	0.16
KHR-10/227.25	0	44.92	2.95		21.36	17.15	4.16	4.43	1.32	0.72
KHR-10/237.80	5.12	41.28	2.95		20.25	20.15		4.67	1	0.76
KHR-10/270.00	5.48	43.11	2.72		16.92	19.5		5.09	3.65	0.74
KHR-10/300.00	8.1	45.53	2.54		20.45	10.83		3.46	5.31	0.51
Max	12.29	57.12	14.90	0.89	21.36	32.17	18.97	6.12	10.99	1.04
Min	0	36.72	2.25	0.46	0.12	6.36	0.53	2.20	1	0.16

Table 5. Rare earth element data (ppm) of mafic rocks of Khor by ICP-OES (n=19)

	La	Ce	Pr	Nd	Sm	Eu	Gd	Tb	Dy	Ho	Er	Tm	Yb	Lu	Y
KHR-1/179.75	18	40	5	20	6	1.7	7	1	5	1	3	<1	2.8	0.5	25
KHR-1/239.80	100	188	20	70	15	4.6	20	2	6	1.3	5	<1	2.9	0.5	32
KHR-1/294.55	208	279	24	69	6	1.4	10	<1	<3	<1	<3	<1	<2	<0.5	10
KHR-3/248.40	18	35	<5	18	6	1.7	7	1	5	1.1	3	<1	2.8	0.5	28
KHR-3/276.05	25	56	7	26	7	2	8	1	5	1.2	3	<1	3	0.5	29
KHR-3/303.15	20	43	5	22	7	2.1	8	1	6	1	3	<1	3	0.5	30
KHR-4/227.15	58	115	13	44	11	3	10	1	5	1	4	<1	2.8	0.5	29
KHR-4/279.75	32	59	6	24	5	1	5	<1	4	1.1	3	<1	2.8	0.5	29
KHR-4/302.80	22	45	5	21	6	1.9	8	1	5	1	3	<1	2.6	0.5	30
KHR-5/252.20	30	55	6	24	6	1.8	8	1	4	1	3	<1	3	0.5	20
KHR-5/293.00	22	48	5	18	5	1.5	7	1	5	1	3	<1	3	0.5	28
KHR-6/114.10	19	42	5	20	6	1.9	8	1	5	1	3	<1	3	0.5	28
KHR-6/276.45	23	46	5	20	6	2	8	1	6	1	3	<1	3	0.5	30
KHR-6/300.05	22	42	5	21	7	2	8	1	5	1.3	4	<1	3	0.5	30
KHR-7/187.05	48	85	9	29	5	1.2	6	<1	<3	<1	<3	<1	<2	<0.5	15
KHR-7/210.00	23	45	5	18	5	1.4	6	<1	5	1	3	<1	3	0.5	25
KHR-7/226.90	22	50	6	25	8	2.6	10	1.2	6	1.4	4	<1	3	0.5	34
KHR-8/259.50	21	50	6	23	7	2.1	8	1	5	1	3	<1	3	0.5	30
KHR-8/264.80	20	42	5	19	6	1.9	7	1	5	1	3	<1	3	0.5	28

(Plate-2e) plot the suite mostly falls in the tholeiitic basalt field. V vs Ti (Plate-2f) plot shows the distribution of the suite (with enhanced Ti content) mostly in the ocean island and alkali basalt fields. Zr vs Zr/Y plot (Plate-2g) indicates the tectonic setting as within plate but Y vs Cr plot (Plate-2h) shows cluster of points in the MORB field. Ternary AFM (Plate-3a) plot shows the distribution of the suite in the tholeiitic field, whereas in MnO-TiO$_2$/10-P$_2$O$_5$ (Plate-3b) and Zr-Ti/100-Sr/2 (Plate-3c) the samples plot in ocean island tholeiite and ocean floor basalt fields respectively. In La/10-Y/15-Nb/8 (Plate-3d) the samples fall broadly in the late- to post orogenic intra-continental domain and in K$_2$O-TiO$_2$-P$_2$O$_5$ (Plate-3e) it dominantly falls in the oceanic field. Rare earth element (REE) data of selected samples of this suite is shown in Table 5 and chondrite-normalised and NMORB normalized plots are shown in Fig.6 and Fig.7 respectively. The plots show that there is a steep slope from light REE to heavy REE, indicating enrichment of the former with respect to the latter and (La/Lu)$_n$ ranging from 3.49-19.38 and (La/Yb)$_n$ ranging from 3.76-20.47 also corroborate it. The enriched light REE and the gentle- to flat heavy REE pattern point towards a primary shallow mantle source (Sharma, 2009) and this is corroborated by the presence of modal and normative olivine. Thus, it is evident that the suite has a complex signature that predominantly points to a primary tholeiitic affinity, but enhanced K$_2$O and TiO$_2$ content tend to impart a slightly alkaline tendency and oceanic affiliation respectively. Summarising the overall geochemical signature, it appears that this suite of rock, of oceanic- to upper mantle origin, was emplaced as an intrusive in a within-plate intra-continental setting, after the formation of Bundelkhand granitoids.
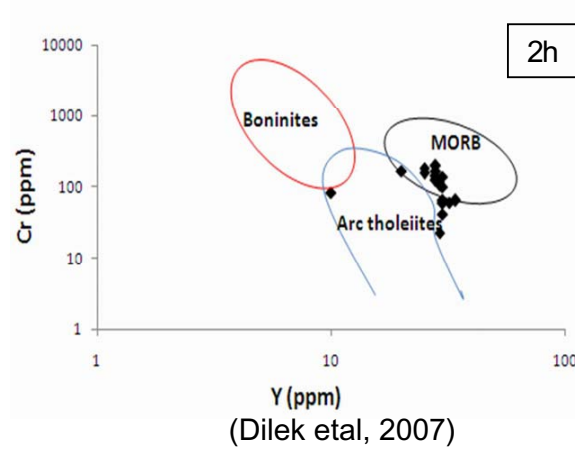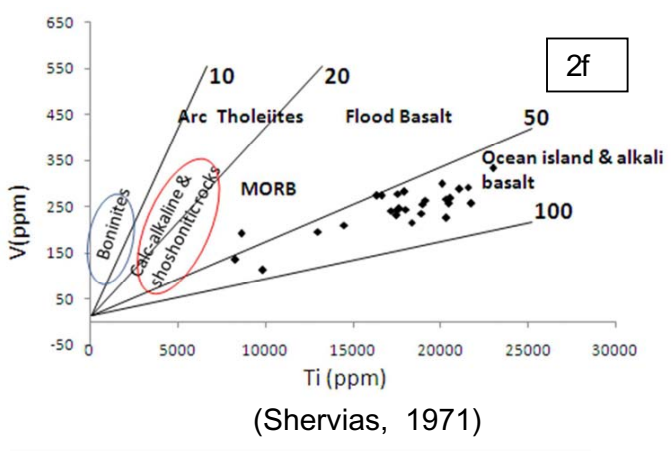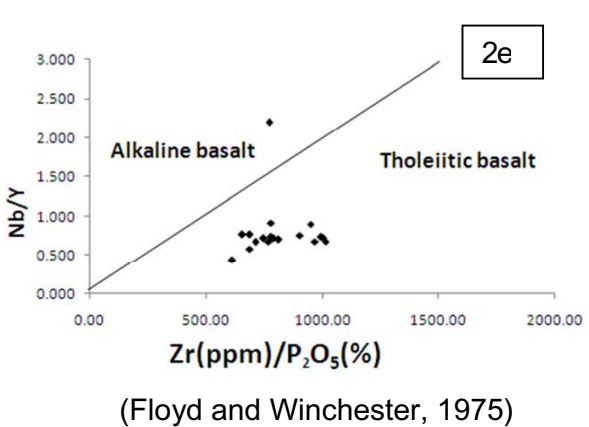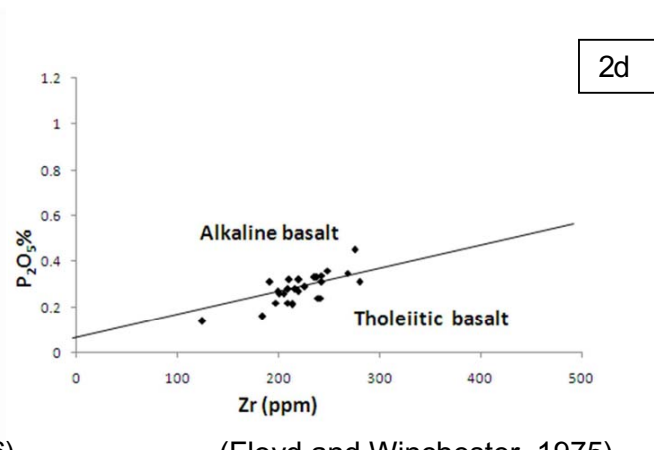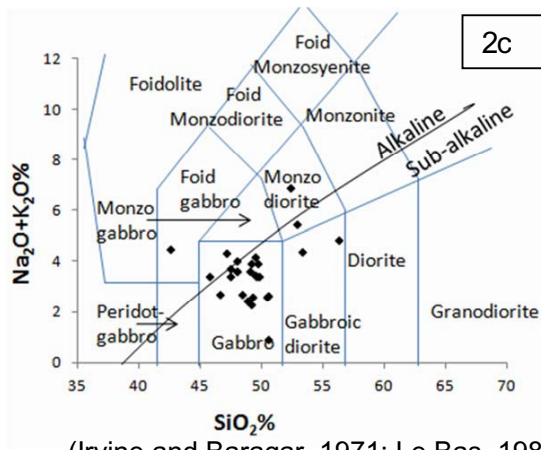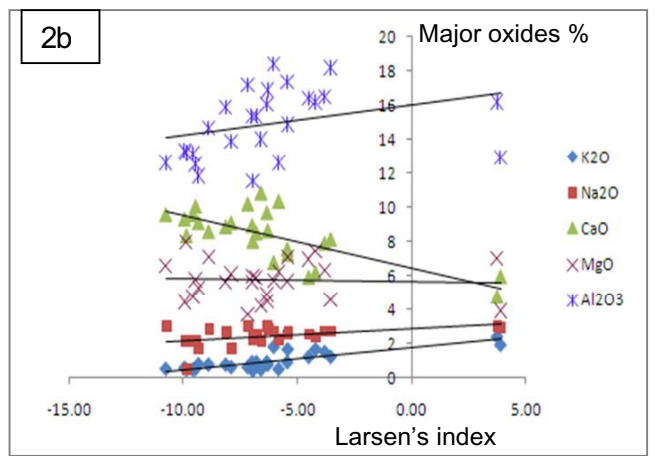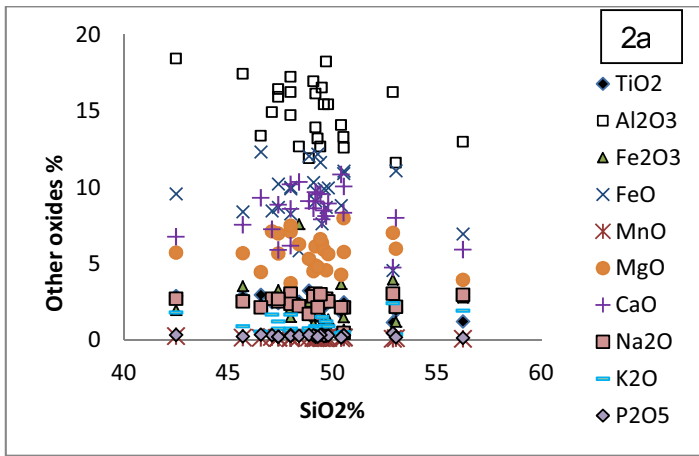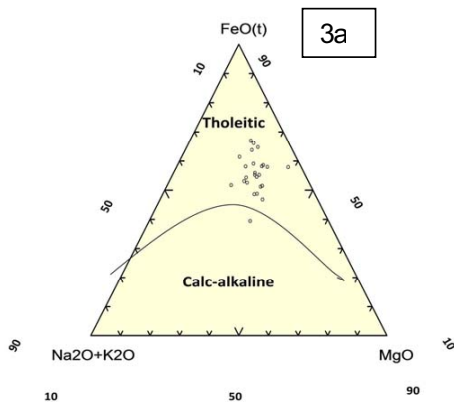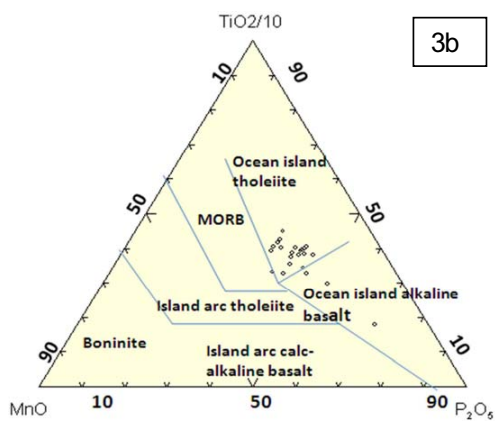
Plate 2. Binary plots of mafic rocks.

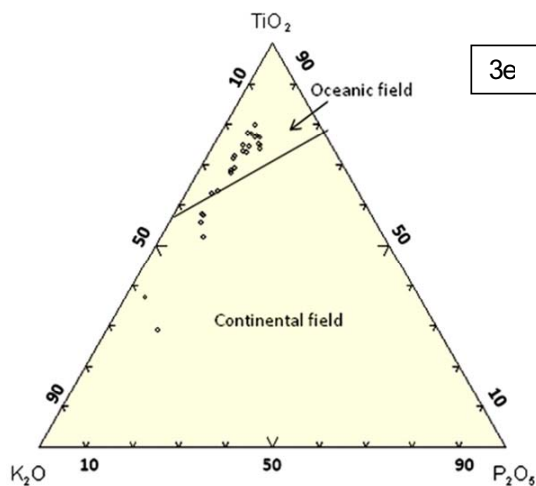(Irvine and Baragar, 1971; Le Bas, 1986)

(Floyd and Winchester, 1975)

(Floyd and Winchester, 1975)

(Shervias, 1971)

(Pierce and Norry, 1979)

(Dilek etal, 2007)

3a

FeO(t)

Tholeiitic

Calc-alkaline

Na2O+K2O   MgO

Irvine and Baragar, 1971

3b

TiO2/10

Ocean island tholeiite

MORB

Island arc tholeiite   Ocean island alkaline basalt

Boninite   Island arc calc-alkaline basalt

MnO   P₂O₅

(Mullen, 1983)

3c

Ti/100

Ocean Floor Basalt

Low-K arc tholeiites

Calc-alkaline basalt

Zr   Sr/2

(Pearce and Cann, 1973)

3d

Y/15

N-MORB
E-MORB
Tholeiites
Calc-alkaline
Alkaline

Orogenic (compressive) domains island arcs, active margins

Late- to post– orogenic (compressive to distentive) Intra continental domains

Anorogenic (distentive) domains

La/10   Nb/8

(Cabanis and Lecolle, 1989)

3e

TiO₂

Oceanic field

Continental field

K₂O   P₂O₅

(Pearce et al, 1975)

Plate 3. Ternary plots of mafic rocks

SIGNIFICANCE OF NORITIC ROCKS IN BUNDELKHAND CRATON

Many noritic intrusions are reported globally in the Neoarchaean and Palaeoproterozoic times, mostly occuring as part of major layered igneous complexes or as dyke swarms (Hall and Hughes, 1990a) and emplaced in an intracratonic rift or hotspot (plume) setting. The Rajasthan craton contains Proterozoic carbonatitic and granitic rocks and old granulites within Delhi metasediments, mainly at Sandmata in the eastern part of the craton. These granulites comprise charnockite-enderbite-mafic granulites associated with norite dykes and are believed to be lower crustal rocks with minor upper mantle admixture. These norite dykes intrude amphibolite or granulite rocks of the banded gneiss complex at various places in Rajasthan, N.W. India and are marked by ophitic to sub-ophitic texture with strongly zoned sub-calcic clinopyroxene and orthopyroxene, olivine and plagioclase, with subsidiary biotite. Sharma (2009) explains the magmatic origin of this suite in a mantle plume-related, hot spot induced, uparched crust that gradually stretched, triggering intra-cratonic rifting, a theory first proposed by Burke and Dewey (1973). Subsequently, due to mantle-underplating, melt derived from upper mantle / lower oceanic crust
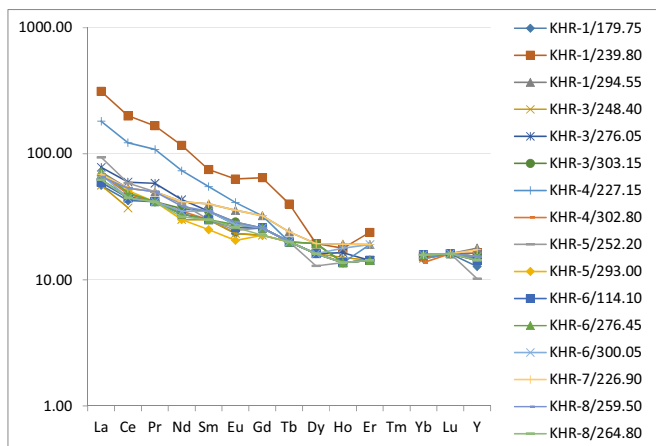
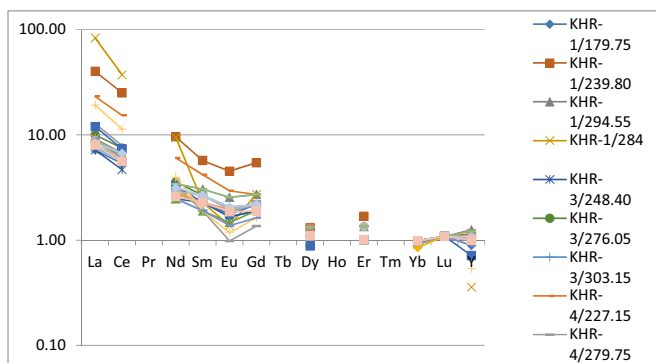**Fig. 6.** Chondrite-normalised (Felsche and Herrmann, 1978) REE plot of mafic rocks from Khor.

Fig.7. NMORB-normalised (Sun and McDonough, 1989) REE plot of mafic rocks from Khor.

on the basement geological history below the Vindhyans in between the two cratons is inadequate. The surfacially exposed and commonly occurring NW-SE trending dolerites dykes within Bundelkhand granitoid are typically tholeiitic basalts with clinopyroxene, plagioclase, magnetite-ilmenite and are quartz normative in nature, while the ultramafics are komatiite or basaltic komatiite in composition and are olivine normative in character. (Rao et al., 2005). In view of the mineralogical presence and normative occurrence of either quartz or olivine in the mafic rocks of Khor, it appears that it has a character intermediate between the tholeiitic dolerite dykes and the komatiite-type ultramafics reported from Bundelkhand craton. The complex geochemical signature of the rocks under study, whereby both intra-continental as well as a mixture of oceanic- to upper mantle signatures are evident and both quartz and olivine normative compositions are observed, may imply involvement of lower crustal- to mantle component juxtaposed on intracratonic rift setting. Srivastava and Gautam (2012) reported high Mg, high silica mafic igneous rocks having similar geochemical composition as norite, emplaced as dykes within granite gneiss in the southern Bastar craton during Neoarchaean times, in an intracratonic rift setting. Rogers (1996) and Rogers and Santosh (2002,2003) discussed existence of an Archaean (~3 Ga) Supercontinent known as "Ur", the configuration of which includes several Indian cratons, viz., Dharwar, Bastar, and Singhbhum, besides the Kalahari craton of southern Africa, the Pilbara craton of western Australia, and the coastal region of East Antarctica. It is possible that the Rajasthan-Bundelkhand cratons also comprised a part of this old Supercontinent and underwent similar Archean geological history as Bastar craton, which is situated to the south of Bundelkhand craton.

A report by Fugro Airborne Surveys Pvt. Ltd. (2008), which carried out airborne geophysical survey (radiometric, magnetic, electromagnetic and resistivity) over part of the western Bijawar massif, of which the study area forms a part, indicates evidence of the granite basement shallowly dipping towards the west, whilst it appears flat lying or shallowly dipping eastwards elsewhere in the survey area (Fig.8). According to the report, the depth-to-magnetic basement shows presence of a NNW–SSE trending escarpment, running approximately 10km from, and sub-parallel to the geophysical survey boundary, possibly indicating the presence of a fault line. The report also indicates that the underlying granite basement surface appears to have undergone change in the attribute in this part and that the sediment thickness increases towards the west (Fig.9).
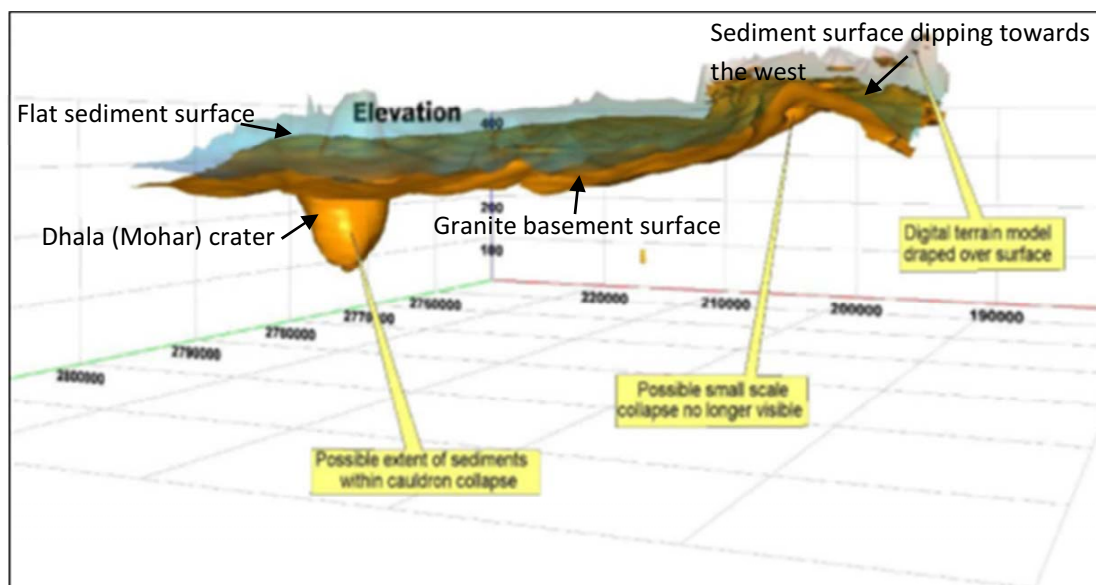
was emplaced within the lower crustal rocks that were transformed into granulites due to the high temperature and the whole assemblage was exhumed along ductile shear zones, during Mesoproterozoic Delhi orogeny. The sub-surface occurrence of the noritic rocks at Khor, situated to the west of Bundelkhand craton, may signify the eastern analog of such an activity recorded in Rajasthan craton, even if separated by a distance of hundreds of kilometers and covered by an enormously thick Vindhyan Supergroup sediments in between. Data

Fig.8. Isosurface generated at 5mS/m. View from the north east. (Modified after report by Fugro Airborne Surveys Pvt. Ltd, 2008)
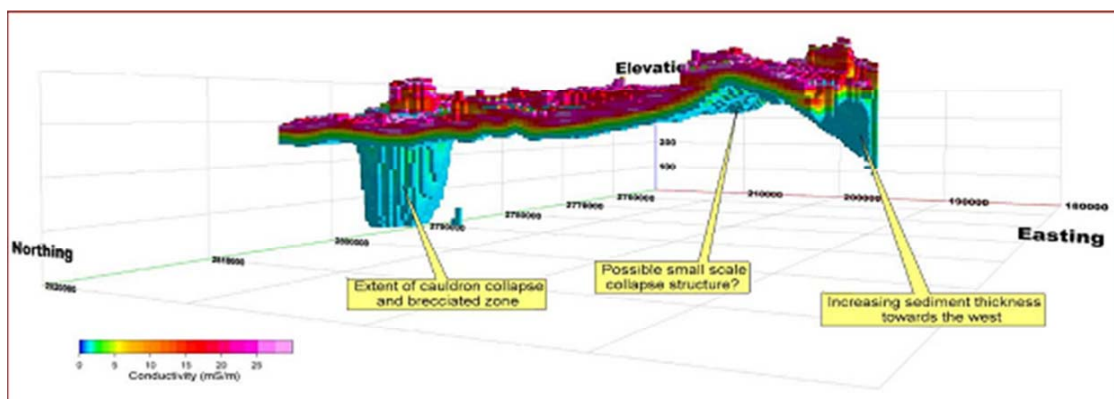
Fig.9. Threshold display of 3-D voxel model. Lower threshold is set at 1mS/m and upper threshold is set at 400mS/m. (Fugro Airborne Surveys Pvt. Ltd, 2008)

CONCLUSION

The extensive studies of sub-surface samples from the western part of Bundelkhand craton, near Khor area, Shivpuri dist., M.P., thus, brings to light unreported occurrence of hypersthene-bearing mafic dyke-like intrusive rocks of noritic composition and largely tholeiitic affinity (with enhanced Ti and K) within Bundelkhand granitoid, which has no surface expression. This suite of rock represents an oceanic component and is of lower crustal- to upper mantle in origin, and appears to have been emplaced in a within-plate intra-continental (intra-cratonic) rift setting, after the stabilisation of the Bundelkhand craton. In analogy with the noritic dykes of Sandmata in Rajasthan block in the west, this body may also be a product of mantle underplating in an adjacent plume-related, hot spot-induced, deep rift environment of an extremely stretched continental crust, during Paleoproterozoic times. Halder and Ghosh (2000) had proposed hot spot generated trilete rift system within the stable Bundelkhand craton during Paleoproterozoic time, resulting in the formation of Bijawar basin and Gwalior basin along the two arms of this rift system, to the south east and north west respectively. The third arm was supposed to be inactive and covered by Deccan traps and other younger rocks. The rift in the present context, occupying the area between Rajasthan craton in the west and Bundelkhand craton in the east, may be coeval with the Aravalli rift setting (Sharma, 2009) and this may have widened and got reactivated with time, eventually causing eastward migration of the Bundelkhand craton which then got separated from the Rajasthan cratonic block in the west during Paleoproterozoics. This may have resulted in the formation of a wide basin, into which the Mesoproterozoic Vindhyan sediments got deposited subsequently. It is not known whether the Vindhyans are underlain by Paleoproterozoic analogs of Aravalli Supergroup in this part, but such analogs are present in the Paleoproterozoic rift-related extensional basins of Bijawar-Sonrai in the southeast and south of Bundelkhand craton and Gwalior basin to the northwest. In fact, it is a very preliminary proposal that there might have been two plume-related, hot spot-induced, deep trilete rift settings (Fig.10) comprising a rift system, operational at the time of formation of Gwalior basin (one arm of the northern rift) and Bijawar-Sonrai basins (one arm of the southern rift). Both these basins were deep and had experienced oceanisation in the form of mafic magmatic activity at the onset of sedimentation. Like Aravalli Supergroup metasediments, the rocks of these basins underwent low grade metamorphism, although structure-wise they are less complex may be due to non-attainment of orogenic culmination. The Vindhyan basin on the other hand, may have resulted by the joining of two arms of the two trilete rifts (southern arm of northern rift and northern arm of southern rift), that eventually
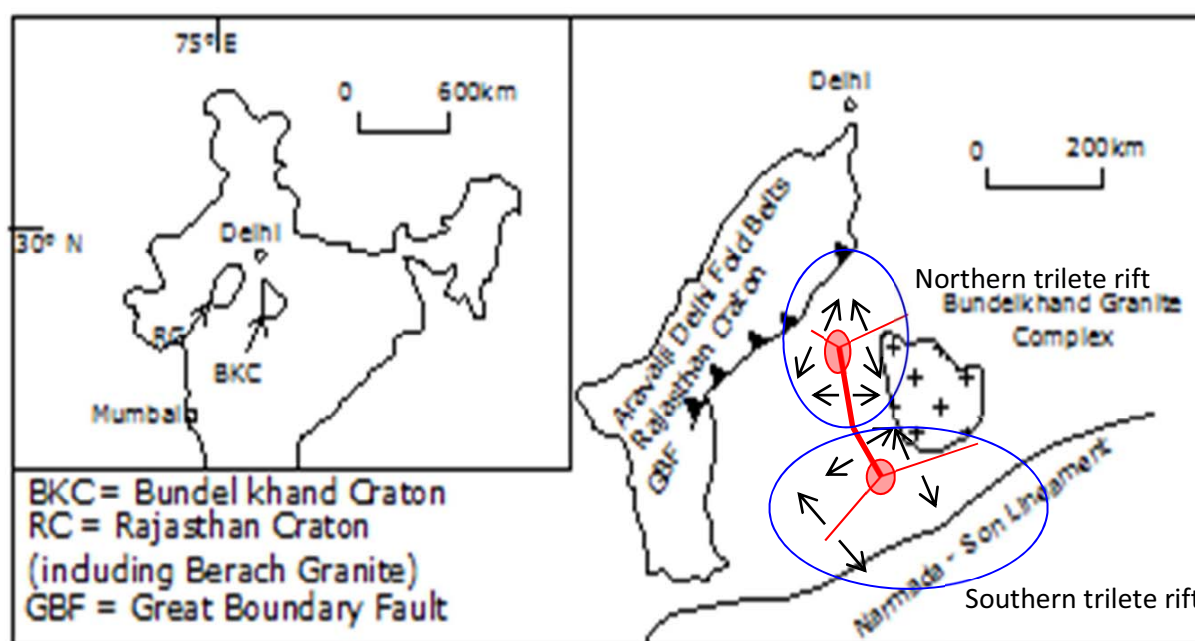

Fig.10. Location of Rajasthan and Bundelkhand cratons (Sharma, 2009) and the hypothetical fossil compound trilete rift system. Dark red joined arms may be the site of present Vindhyan basin and red spots are plumes.

became inactive possibly without undergoing orogenesis (unlike Delhi Supergroup metasediments). Inactive rift-related sediments, like those of the Vindhyan Supergroup, generally comprise orthoquartzite (quartz-arenite)-carbonate-shale suites (Kale, 1991) and are characterized by lack of structures and metamorphism. Such basins signify "Atlantic-type" passive continental margin system that develops under extensional tectonic regimes on the trailing edges of continental blocks (Park, 1988).

Whether the fact inferred by geophysical survey about the sudden change in the attribute of the Bundelkhand granitoid towards the west in the study area, has any bearing on the possibility of the existence of such an ancient fossil intracratonic rift environment, in which noritic intrusions took place at many places during late Archean to Paleoproterozoic, remains to be ascertained. The enormous thickness of Middle Proterozoic unmetamorphosed, undeformed Vindhyan sediments deposited between western margin of the Bundelkhand craton, and eastern margin of Rajasthan craton, keeps such a possibility alive. The geological, petrological and geochemical findings of this study give strong indication in favour of the above possibility and strengthens the concept of a single protocontinent known as Rajasthan-Bundelkhand craton. However, this hypothesis can be conclusively established by the geochronological data of all norites in Bundelkhand and its surrounding cratons.

References

Bowen, N.L. (1928) Evolution of the igneous rocks, Princeton University Press, Princeton, 334p.

Burke, K. and Dewey, J. F. (1973) Plume generated triple junctions: key indicators in applying plate tectonics to old rocks: Jour. Geol., v.81, pp.406–433.

Cabanis, B., and Lecolle, M. (1989) Le diagramme La/10-Y/15-Nb/8: un outil pour la discrimination des series volcaniques et la mise en evidence des processus de melange et/ou de contamination crustale, C. R. Acad. Sci. Ser. 2, v.309, pp.2023-2029.

Dilek, Y., Furnes, H. and Shallo, M. (2007) Suprasubduction zone ophiolite formation along the periphery of Mesozoic Gondwana, Gondwana Res., v.11, pp.453–475.

Felsche, J., and Hermann, A.G. (1978) Yttrium and lanthanides, chapter 39, *In:* Wedepohl, K.H. (Ed.), Handbook of Geochemistry: Verlin, Springer-Verlag, v.2(5), pp.57-71.

Floyd, P.A. and Winchester, J.A. (1975) Magma type and tectonic setting discrimination using immobile elements, Earth Planet. Sci. Lett., v.27, pp.211-218.

Fugro Airborne Surveys Pty Ltd, Australia (2008) Geophysical Interpretation report of Mohar area, Shivpuri dist., M.P, Unpublished.

Haldar, D. and Ghosh, R.N. (2000) Eruption of Bijawar lava: An example of Precambrian volcanicity under stable cratonic condition, Proceedings volume. Int. Sem. Precambrian crust in Eastern and Central India, IGCP-368, Bhubaneshwar, India, pp.151-170.

Hall, R.P. and Hughes, D.J. (1990a) Noritic magmatism. *In:* R.P. Hall and D.J. Hughes (Eds.), Early Precambrian Basic Magmatism. Blackie, Glasgow, pp.83-110

Irvine, T.N. and Baragar, W.R.A. (1971) A guide to the chemical classification of the common volcanic rocks. Canadian Jour. Earth Sci., v.8, pp.523-548.

Kale, V. (1991) Constraints on the evolution of the Purana basins of peninsular India. Jour. Geol. Soc. India, v.38, pp.231-252.

Kuno, H. (1959) Origin of Cenozoic petrographic provinces of Japan and surrounding areas, Bull. Volcanol., v.20, pp.37-76.

Larsen, E.S. (1938) Some new variation diagrams for groups of igneous rocks. Jour. Geol., v.46, pp.505-520.

LeBas, M.J., LeMaitre, R.W., Streckeisen, A. and Zanettin, B. (1986) A chemical classification of volcanic rocks based on the total alkali-silica diagram. Jour. Petrol., v.27, pp.745-750.

Meert, J.G., Pandit, M.K., Pradhan, V.R., Banks, J.,Sirianni, R., Stroud, M., Newstead, B. and Gifford, J. (2010) Precambrian crustal evolution of Peninsular India: A 3 billion year odyssey Jour. Asian Earth Sci., v.39, pp.483-515.

Mondal, M.E. A. and Ahmad, T. (2001) Bundelkhand mafic dykes, central Indian shield: implications for the role of sediments subduction in Proterozoic crustal evolution. Island Arc, v.10, pp.51-67.

Mullen, E.D. (1983) $MnO/TiO_2/P_2O_5$: a minor element discriminant for basaltic rocks of oceanic environments and its implications for petrogenesis. Earth Planet. Sci. Lett., v.62, pp.53-62.

Park, R.G. (1988) Geological structures and moving plates, Glassgow, Blackie, 337p.

Pearce, J.A. and Canne, J.B. (1973) Tectonic setting of basic volcanic rocks determined using trace element analyses. Earth Planet. Sci. Lett., v.19, pp.290-300.

Pearce, J.A. and Norry, M.J. (1979) Petrogenetic implications of Ti, Zr, Y and Nb variations in volcanic rocks. Contrib. Mineral. Petrol., v.69, pp.33-47.

Rao, Mallikarjun, J., Pooranchandra Rao, G.V.S., Widdowson, M. and Kelley, S.P. (2005) Evolution of Proterozoic mafic dyke swarms of the Bundelkhand granite massif, central India. Curr. Sci., v.88(3), pp.502-506.

Rogers, J.J.W. (1996) A history of continents in the past three billion years. Jour. Geol., v.104, pp.91-107

Rogers, J.J.W. and Santosh, M. (2002) Configuration of Columbia, A Mesoproterozoic supercontinent. Gondwana Res., v.5(1), pp.5-22.

Rogers, J.J.W. and Santosh, M. (2003) Supercontinents in earth's history, Gondwana Res., v.6(3), pp.357-368.

Sharma, R.S., Sills, J.D. and Joshi, M. (1987) Mineralogy and metamorphic history of norite dykes within granulite facies gneisses from Sand Mata, Rajasthan, NW India. Mineral. Magz., v.51, pp.207-215.

Sharma, R.S. (2009)Cratons and fold belts of India. Springer, 304p.

Shervais, J.W. (1982) Ti-V plots and the petrogenesis of modern and ophiolitic lavas. Earth Planet. Sci. Lett., v.59(1), pp.101-118.

Srivastava, R.K. and Gautam, Gulab, C. (2012) Early Precambrian mafic dyke swarms from the Central Archaean Bastar Craton, India: geochemistry, petrogenesis and tectonic implications. Geol. Jour., v.47, pp.144-160.

Sun, S.-s. and McDonough, W.F. (1989) Chemical and isotopic systematics of oceanic basalts: implications for mantle composition and processes. Geol. Soc. London Spec. Publ., v.42, pp.313-345.

Wager, L.R and Deer, W.A. (1939) Geological investigations in East Greenland, Part 3. The petrology of the Shaergaard intrusion, Kangerdludssuaq, East Greenland, Medd. Gronl., v.105(4), pp.1-352.